Received: 24 June 2021 | Revised: 11 October 2021 | Accepted: 8 November 2021

DOI: 10.1096/fba.2021-00073

RESEARCH ARTICLE

FASEB BioAdvances WILEY

Critical cysteines in the functional interaction of adenylyl cyclase isoform 6 with Gαs

Anjali Y. Bhagirath[1,2] | **Vikram Bhatia**[1,2] | **Manoj Reddy Medapati**[2] | **Nisha Singh**[2] | **Martha Hinton**[1,3] | **Prashen Chelikani**[1,2] | **Shyamala Dakshinamurti**[1,3,4]

[1]Biology of Breathing Theme, Children's Hospital Research Institute of Manitoba (CHRIM), Winnipeg, Manitoba, Canada

[2]Department of Oral Biology, University of Manitoba, Winnipeg, Manitoba, Canada

[3]Department of Physiology and Pathophysiology, University of Manitoba, Winnipeg, Manitoba, Canada

[4]Department of Pediatrics, University of Manitoba, Winnipeg, Manitoba, Canada

Correspondence
Shyamala Dakshinamurti, Section of Neonatology, Department of Pediatrics, Women's Hospital, University of Manitoba, WN 2618-820 Sherbrook St., Winnipeg, MB, Canada R3A1R9.
Email: shyamala.dakshinamurti@umanitoba.ca

Funding information
Heart and Stroke Foundation of Canada; Research Manitoba/Children's Hospital Foundation of Manitoba

Abstract

Activation of adenylyl cyclases (ACs) by G-protein Gαs catalyzes the production of cyclic adenosine monophosphate (cAMP), a key second messenger that regulates diverse physiological responses. There are 10 AC isoforms present in humans, with AC5 and AC6 proposed to play vital roles in cardiac function. We have previously shown that under hypoxic conditions, AC6 is amenable to post-translational modification by nitrosylation, resulting in decreased AC catalytic activity. Using a computational model of the AC6–Gαs complex, we predicted key nitrosylation-amenable cysteine residues involved in the interaction of AC6 with Gαs and pursued a structure–function analysis of these cysteine residues in both AC6 and Gαs. Our results based on site-directed mutagenesis of AC6 and Gαs, a constitutively active Gαs, AC activity, and live cell intracellular cAMP assays suggest that Cys1004 in AC6 (subunit C2) and Cys237 in Gαs are present at the AC–Gαs interface and are important for the activation of AC6 by Gαs. We further provide mechanistic evidence to show that mutating Cys 1004 in the second catalytic domain of AC6 makes it amenable to inhibition by Gαi, which may account for decreased functional activity of AC6 when this residue is unavailable.

KEYWORDS

adenylyl cyclase, cyclic AMP, cysteine, G proteins, mutational analysis

1 | INTRODUCTION

Pulmonary vasodilation is mediated by endothelial nitric oxide acting via the cyclic guanosine monophosphate pathway, and by circulating prostacyclin acting through the cyclic adenosine monophosphate (cAMP) pathway. Persistent pulmonary hypertension of the newborn is a syndrome characterized by disruption of circulatory

Abbreviations: AC, adenylyl cyclase; ANOVA, analysis of variance; CAM, constitutively active mutant; cAMP, 3′, 5′-cyclic adenosine monophosphate; DM, *N*-dodecyl β-D-maltoside; FACS, fluorescence activated cell sorting; FBS, fetal bovine serum; FSK, forskolin; Gαi, inhibitory guanine nucleotide regulatory protein; Gαs, stimulatory guanine nucleotide regulatory protein; HTRF, homogeneous time-resolved fluorescence; IP, immunoprecipitation; PBS, phosphate-buffered saline; SDS-PAGE, sodium dodecyl sulfate-polyacrylamide gel electrophoresis; SEM, standard error of the mean.

adaptation at birth, resulting in varying degrees of hypoxic respiratory failure.[1] The ensuing hypoxemia and metabolic acidosis start a vicious cycle of increased pulmonary vascular resistance and further hypoxemia, with often fatal outcomes. Pulmonary and cardiac tissues are often hypoxic at the time of therapeutic intervention, which may impair responsiveness to vasodilator therapy.[2–5] Hypoxia is known to attenuate the sensitivity of pulmonary arterial adenylyl cyclase (AC) to prostacyclin[6] or β-adrenergic stimulation.[7]

The AC–Gαs–cAMP pathway is a key pathway for pulmonary vasodilation and cardiac contraction. Binding of Gαs to AC results in the generation of intracellular cAMP.[8] ACs are ubiquitously expressed, plasma membrane associated proteins consisting of six transmembrane domains and two cytosolic catalytic domains (C1 and C2). The nine membrane-bound AC isoforms share a common topology.[9,10] The cytoplasmic domains of AC create a pseudo-symmetrical site that is primed for bidirectional regulation by either the stimulatory or inhibitory G proteins. Despite their topographical similarity, each isoform displays varying degrees of structural similarity and distinct patterns of regulation; AC isoforms 5 and 6 can be activated by GTP-activated Gαs[11,12] as well as by allosteric activator forskolin,[13] and are inhibited by Gαi.[14,15]

We previously demonstrated the predominance of AC isoform 6 expression in pulmonary arterial myocytes.[16] AC6 catalytic activity is known to be attenuated by nitric oxide[17]; and under hypoxic conditions is inhibited due to S-nitrosylation,[16] a reversible post-translational modification of proteins that can occur during hypoxia,[18] targeted at specific cysteines.[19,20] As nitrosylation occurs only on specific cysteine residues, this also implicates cysteine residues in AC6 activation.

Cysteines are the least abundant residues in proteins, but also the most conserved, critical to structure and function. Analysis of the primary structure of different AC isoforms demonstrates some highly conserved cysteine residues within the most conserved parts of the catalytic site. The long history of examination of the structure of AC catalytic domains has been largely derived from the crystal structure of AC5 and AC2 catalytic subunits, and recently the AC9 holoenzyme.[21–23] The juxtaposition of the catalytic C1 and C2 domains, forming a functional heterodimer, is altered by the interaction of AC with Gαs, resulting in AC catalytic activity. Cysteines located at positions 432, 441 and 444 in the C1 domain of rat AC5 were identified to be involved in its binding to the second catalytic domain as well as to its substrate ATP.[22] These C1 cysteines, plus C441 located in C2 also participate in the formation of the allosteric forskolin binding pocket.[22] In AC5, C459 and C494 are important for the coupling of the two catalytic domains and thereby enzyme activation.[22] Studies of the AC–Gαs interface have mapped their contact surfaces; the switch II helix of Gαs (residues 225–240) inserts into the groove between the α2′ helix and the α3′–β4′ loop of AC C2, with the majority of interacting amino acids located on β4′.[24] In AC2, C911 located at the edge of the α2′ helix in C2 was identified as adjacent to residues directly interacting with Gαs, and important in the binding of C2 to C1[22]; but its role in securing the Gαs interaction was not characterized functionally. Examination of the Gαs binding pocket in AC5 and AC6 identified residues phenylalanine 1078 and serine 1090 as involved in activation.[25] While several studies have noted that blocking or modifying cysteine thiol groups, using reagents such as *N*-ethylmaleimide, and 5,5′-dithobis (2-nitrobenzoic acid), can dose-dependently inhibit AC activity,[26–29] the role of cysteines in AC6–Gαs docking has not been directly examined.

While there is a range of sequence conservation for the catalytic domains among the various AC isoforms, they respond to hypoxia differently[16] and also demonstrate differential responses to stimulatory and inhibitory G proteins[15] as well as other regulatory proteins.[30,31] Given the key role of AC6 in pulmonary hypertension and its susceptibility to inhibition, we hypothesized that the blockage of specific cysteines in AC6 could abrogate its activation by Gαs. We previously published a homology model for the AC6–Gαs complex and identified highly conserved residues in both AC6 and Gαs, predicted to play a role in their interaction.[32] Using the recently reported cryo-electron microscopy structure for the bovine AC9–Gαs complex,[21] we identified two critical cysteine residues with a high probability for nitrosylation in our human AC6–Gαs homology model: C1004 in a conserved region of the AC-C2; and C237 on Gαs, at its interface with AC6. These two cysteines appear to form the first point of contact for Gαs docking with AC. In this study, we perform site-directed mutational analysis of these cysteines in AC6 and in Gαs, to examine their functional roles in AC6–Gαs interaction and AC activation. To avoid the need for receptor-mediated activation of Gαs, a constitutively active mutant (CAM) of Gαs, with the well-described mutation Q227L slowing its GTPase activity,[33,34] was used as a base. We then examined the roles of cysteines C1004 in AC6, and C237 in Gαs CAM, in determining AC catalytic activity and intracellular cAMP generation, and in the critical regulatory balance of AC6 activation by Gαs versus inactivation by Gαi.

2 | MATERIALS AND METHODS

The human embryonic kidney (HEK293T) cell line was purchased from ATCC. Dulbecco's Modified Eagle

Medium (DMEM)-F12 (Gibco, Life Technologies), 10% (v/v) heat-inactivated fetal bovine serum (FBS; Sigma), and 1% (v/v) penicillin–streptomycin (Gibco, Life Technologies) were used in a complete cell culture medium. Hygromycin (200 μg/ml; Sigma-Aldrich) was used in the selection medium to generate AC6 stable cells. Zeocin (100 μg/ml; Thermo Fisher Scientific) was used in the selection medium to generate Gαs WT and CAM stable cells.

DMEM/F12, FBS, penicillin–streptomycin, Lipofectamine 2000, and Opti-MEM, were acquired from Thermo Fisher Scientific. *N*-Dodecyl β-D-maltoside (DM) was purchased from Sigma-Aldrich (Cat #D4641). The CAMP-Glo Max assay kit (Cat #V1681) was obtained from Promega. Gαi-based cAMP homogeneous time-resolved fluorescence (HTRF) kit was obtained from Cis bio (Cat# 62AM9PEB). Gαi inhibitor, Tat-GPR was purchased from Kerafast (Cat# ESC101). APC anti-FLAG tag antibody (Cat #637308) and anti-HA-Alexa Fluor 488 antibody (Cat #901509) were purchased from Biolegend; anti-HA tag antibody from Genscript (ab18181); anti-FLAG antibody from abcam (ab245895). Gαs antibody was purchased from Proteintech (Cat #17903-1AP); Gαi antibody from Santa Cruz (sc-7276) and native AC6 antibody from abcam (ab 14781).

For co-immunoprecipitation (IP), Anti-HA magnetic beads were purchased from Thermo scientific (Cat #88836), Anti-FLAG M2 magnetic beads were purchased from Sigma (Cat #M8823), magnetic anti-IgG beads were purchased from Cell Signaling Technologies (Cat #5873). Protease inhibitors and common chemicals were purchased from either Fisher or Sigma.

2.1 | Molecular modeling of AC6 and Gαs complex

The cryo-electron microscope structure of the bovine AC9–Gαs complex was recently reported for the full-length AC9 isoform.[21] We performed Clustal Omega pairwise sequence alignment to check the homology between the human AC6 and AC9, as well as the human AC6 and bovine AC9. We then built a molecular model of AC6–Gαs complex protein using the available AC9-Gαs cryoEM (PDB ID: 6R3Q) structure as a template on the Maestro platform (Schrodinger Maestro v11 suite). To check the other templates, the amino acid sequences of AC6 (UniProtKB-O43306) and Gαs (UniProtKB-P63092) were submitted to the I-TASSER server (https://zhanglab.ccmb.med.umich.edu/I-TASSER/). The server gives ten templates using the LOMETS meta-server threading approach, which performs the multiple template alignment from the PDB library. Model number 6R3Q was found to be one of the best, with a high template modeling score (TM, which assesses the topological similarities of protein structures). After building the homology model, a protein preparation wizard was performed in Maestro to fill the missing side chains and loops. The loops of side chains of the AC6–Gαs structure were further refined by loop refinement. The model was energy minimized according to Maestro guidelines by selecting all atoms and performing 65 steps per iteration with 0.01 kcal/mol/Å root-mean-square (RMS) gradient for convergence using the PRIME module of Schrodinger software. The model‘s quality was checked using Procheck (https://servicesn.mbi.ucla.edu/PROCHECK/).[35] Ramachandran plot showed 99.1% of residues were in favorable and allowed regions. The complex of AC6–Gαs was further analyzed to study the interaction using PyMol molecular visualization software.

2.2 | Recombinant plasmid DNA and transfections

Using a targeted substitution mutagenesis approach to reveal the function of a cysteine's reactive thiols without altering residue bulk or hydrophilicity, human AC isoform six wild-type (AC6 WT) and AC6 containing alanine substitutions at positions C1004, C1145, or C447, as well as the Gαs wild-type (Gαs WT), and Gαs (Q227L) CAM mutant with or without cysteine-to-alanine substitution mutations at C162, C174, and C237, were codon-optimized for expression in the mammalian cells, and commercially synthesized (GenScript Inc.) as previously described.[36] All the cysteine-to-alanine mutations in Gαs were made in the CAM (Gαs CAM), and are designated as Gαs CAM (C162A), Gαs CAM (C174A), and Gαs CAM (C237A).

The AC6, Gαs WT, and mutant gene sequences consisted of a FLAG and HA epitope coding sequence at the 5′ and 3′-end genes, respectively. These plasmids were cloned into a mammalian expression vector, pcDNA3.1-Hygro (+) for AC6 and pcDNA 3.1-Zeo (+) for Gαs. HEK293T cells were maintained in DMEM/F12 (1:1) media supplemented with 10% FBS, 100 U/ml penicillin, and 0.1 mg/ml streptomycin at 5% CO_2 and 37°C. HEK293T cells were transfected with 3 μg of DNA per 5×10^6 cells using Lipofectamine 2000 in six-well plates. The wild-type AC6 and CAM mutants were transiently or stably expressed in HEK293T cells using protocols as described previously.[36–38]

2.3 | Flow cytometry

HEK293T cells stably expressing AC6–FLAG, AC6 (C1004A)–FLAG, and/or Gαs–HA were used to detect

expression using a BD FACS canto analyzer. Briefly, 100,000 cells were washed using ice-cold fluorescence activated cell sorting (FACS) buffer (0.5% bovine serum albumin in 1× phosphate-buffered saline [PBS]), followed by fixation with 4% paraformaldehyde. Cells were then permeabilized with 0.2% saponin in FACS buffer and incubated with mouse monoclonal APC conjugated anti-FLAG antibody (1:300 dilution) and/or rabbit monoclonal Alexa Fluor 488-anti-HA antibody (1:300 dilution) for 1 h on ice. HEK293T with APC and Alexa Fluor 488 conjugated IgG antibody were used as negative control. The cells were then washed thrice with FACS buffer and were resuspended in 200 μl of the same. The fluorescent intensity was measured using a BD FACS Canto analyzer and quadrant gating was used to identify the percentage of cells expressing AC6–FLAG and/or Gαs–HA.

2.4 | Determination of intracellular cAMP

The cAMP assays were carried out in HEK293T stably or transiently expressing AC6 or Gαs using a live cell cAMP assay kit (cAMP GloMax Kit Promega) per manufacturer's instructions. Briefly, 24 h after transient transfection, 20,000 cells (96-well white transparent bottom plate) were used for a cAMP assay, in the presence or absence of 10 μM forskolin for 15 min. Luminescence was measured using a FlexStation 3 microplate reader (Molecular Devices). The assays were carried out 3–5 times each and data were analyzed using PRISM software version 8 (GraphPad Software, Inc.); cAMP values were expressed in nM.

Gαi-based cAMP accumulation was measured using an HTRF-based cAMP kit (CisBio) as described previously.[39,40] To measure Gαi-mediated inhibition, 2500 cells/well were added in triplicate wells in white 96-well plates (low volume white microplate, CisBio) in the absence or presence of 3 mM forskolin. The detection range of the HTRF-based cAMP kit is 150–718,000 pM. Cells were treated for 20 min with 100 nM of Gαi inhibitor peptide Tat-GPR (TMGEEDFFDLLAKSQSKRMDDQRVDLAK), as per the manufacturer's recommendation and previous use.[41,42] Isobutylmethylxanthine (IBMX) (100 μM) was included to prevent cAMP degradation during 30 min stimulation on a plate shaker at room temperature. HTRF was measured using a Flex station 3 plate reader (Molecular Devices). Fluorescence resonance energy transfer (FRET) ratios (665/615 nm) were extrapolated to cAMP concentrations using a standard curve according to the manufacturer's instructions.

2.5 | Cell harvesting, cell lysis, and membrane preparation

The membranes were prepared from HEK293T cells stably expressing AC6 WT and mutants using previously published protocols.[43] The high confluent culture plates were kept on ice prior to harvesting, rinsed twice with cold (PBS), then cells were collected by scraping and centrifuging at 500 *g* for 5 min at 4°C. The cell pellets were then resuspended in 5 ml of lysis buffer (10 mM Tris-HCl, pH 7.4 containing protease inhibitors), poured into a 15-ml dounce tissue homogenizer (Kinematica), and homogenized twice with 30 strokes each. The suspension was centrifuged at 300 *g* for 10 min, and the pellet was discarded. The supernatant was then centrifuged at 48,000 *g* for 40 min. The resulting pellet was resuspended in 10 ml of buffer (50 mM Tris-HCl [pH 7.4], 12.5 mM $MgCl_2$, containing protease inhibitors), and the suspension again centrifuged at 48,000 *g* for 40 min. The resulting pellet was resuspended in 1 ml of the suspension buffer (20 mM Tris-HCl [pH 7.4], 500 mM NaCl, 10% glycerol, 1% DM, and protease inhibitors), and aliquots of the suspension were snap-frozen and stored at −80°C.

For obtaining total cells lysates, cells were collected in ice-cold PBS. The cells were then resuspended in lysis buffer (50 mM Tris-HCl [pH 7.4], 12.5 mM $MgCl_2$, containing protease inhibitors) followed by lysis by sonication (Branson Sonifier 450), then centrifuged at 10,000 *g* for 15 min to clear the lysate. The protein concentration was determined using a modified DC protein assay kit from Bio-Rad Laboratories.

2.6 | Western blot analysis

Membrane enriched extracts and whole cell extracts were fractionated by sodium dodecyl sulfate-polyacrylamide gel electrophoresis and transferred to a polyvinylidene difluoride membrane using a transfer apparatus according to the manufacturer's protocols (Bio-Rad). For AC6–FLAG detection, after transferring, the membranes were first blocked by incubation with 5% non-fat milk in TBST (10 mM Tris, pH 8.0, 150 mM NaCl, 0.5% Tween 20) for 60 min, the membrane was washed once with TBST and incubated with antibodies against FLAG (1:1000), hAC6 (1:1000), Gαs (1:1000), Gαi (1:1000), HA(1:1000), or β-actin (1:10,000) at 4°C for 12 h. Membranes were washed thrice with TBST for 10 min and incubated with a 1:3000 dilution of horseradish peroxidase-conjugated anti-mouse or anti-rabbit secondary antibodies for 2 h. Blots were washed with TBST three times and developed

with the ECL system (Bio-Rad) according to the manufacturer's protocols.

2.7 | AC activity

Adenylyl cyclase activity assay was performed as described previously.[16,44] HEK 293T cells stably or transiently expressing AC6 WT, Gαs WT, or Gαs CAM as well as their respective cysteine mutants were lysed in 20 mM Tris buffer pH 7.4 containing protease inhibitors. Lysates were adjusted to 3 μg protein/μl and AC activity assay was carried out in 96-black-well plates with serial wells holding 50 μl of 3 mM ATP and 50 μl of terbium-III norfloxacin (0.5 and 0.1 mM respectively) with 10 mM $MgCl_2$, 20 μM $CaCl_2$ and 1% bovine serum albumin in 20 mM Tris-HCl, at 37°C. The reaction was initiated by addition of 50 μl lysate. Fluorescence intensity of terbium-norfloxacin was acquired by FlexStation3 (Molecular Devices; 337 nm excitation, 545 nm emission) and these experiments were performed three times in triplicate. Baseline fluorescence due to the immediate ATP binding to terbium-norfloxacin decreases only after the addition of AC-containing lysate. This AC-specific activity is measured by the loss of ATP-bound terbium-norfloxacin fluorescence due to ATP-to-cAMP conversion[44] and is represented as Δ fluorescence/min/mg protein.

2.8 | AC6–Gαs/Gαi co-IP

For AC6–Gαs co-IP, FLAG-tagged AC6 and HA-tagged Gαs, or HA-tagged Gαs CAM were co-expressed in HEK293T cells. The cells were lysed using previously described protocols with minor modifications.[45] Briefly, the cells were washed twice with ice-cold PBS and resuspended in lysis buffer (50 mM Tris-HCl, pH 7.4, supplemented with protease inhibitors) followed by sonication (three cycles of 15 s each), and clarification by centrifugation at 15,000 *g* for 10 min at 4°C. For examination under reducing conditions, cells were collected into preboiled reducing lysis buffer with 50 mM Tris and 70 mM β-mercaptoethanol as a reducing agent and boiled for 10 min before addition of cold RIPA buffer, incubation on ice for 15 min, and clarification by centrifugation.[46] For all co-immunoprecipitation studies, 250 μg total protein was then incubated with 40 μl of anti-DYKDDDDK antibody bound beads and anti-HA beads at 4℃ overnight. Mouse anti-IgG beads were incubated with the same amount of total protein as a negative control. Similarly, for AC6–Gαs/Gαi pulldown assay, AC6 WT and mutant cells were first collected in ice-cold PBS. Cell lysates were prepared as described before and 250 μg of total proteins were incubated with 40 μl of anti-DYKDDDDK antibody bound beads at 4℃ overnight.

The immunoprecipitated proteins on beads were washed three times with lysis buffer and solubilized in Laemmli sample buffer (no β-mercaptoethanol). β-mercaptoethanol was added to lysates just prior to loading the gels. For AC6–Gαs co-IP assay, the membranes were probed for both FLAG and HA. For AC6–Gαs/Gαi pulldown the membrane was probed with FLAG for AC6, as well as bound endogenous Gαs and Gαi using respective antibodies.

2.9 | Statistical analysis

Statistical analyses were performed using GraphPad Prism version 6.0 software. One-way analysis of variance and Dunnett's multiple comparison tests were used to determine statistically significant differences in experiments involving more than two treatment groups. Student's *t*-test was used to determine statistical differences in experiments with two treatment groups. Statistical analysis was performed from a minimum of three independent experiments to determine statistical significance wherever applicable. $*p < 0.05$, $**p < 0.01$, $***p < 0.001$; ns is non-significant.

3 | RESULTS

3.1 | Computational model of AC6–Gαs interaction

A pairwise sequence alignment showed 23.9% sequence homology between human AC6 and AC9, whereas 33% similarity was observed between the human AC6 and bovine AC9. To characterize AC6 interaction with Gαs, we built a 3D structure of the AC6–Gαs complex protein using a homology modeling approach, with the known bovine AC9-Gαs cryoEM structure as a template.[21] The AC6–Gαs interaction is predicted to occur in the second catalytic domain of AC6 and is relevant to cAMP production. AC6 structure from the N to C termini can be divided into four main regions: the six TM domains (TM1–TM6), a cytosolic region that includes a catalytic domain (C1a and C1b), followed by the second TM region (TM7–TM12), and then the second cytosolic catalytic domain (C2a and C2b). The most conserved portions are the C1a and C2a domains, which belong to the class III nucleotidyl cyclases. We have not included forskolin in the computational model because it is known to bind at an allosteric site with no influence on Gαs binding. We have also not included any modifications to Gαs.

The computational structure showed Gαs predominantly interacts with the catalytic domain C2 of AC6. The C1004 residue is present at the C2 catalytic domain close to the Gαs–protein interface. Our previously published sequence analysis showed that C1004 in the motif "ANNEGVE**C**LRLLNEI" might play an important role in AC6 structure and function.[32] In the newly built model, C237 residue in Gαs is the closest cysteine at the AC6–Gαs interface, and the distance between the residues C1004 in AC6 and C237 in Gαs is estimated at 7.7 Å (Figure 1A). Based on this model, we hypothesized that these two cysteine residues, AC6 (C1004) and Gαs (C237), might interact reversibly or form a disulfide bridge facilitating AC activation. To delineate the roles of these specific cysteines, we also chose to mutate one cysteine close to the site of interaction (C1145), and one cysteine farther from the site of interaction (C447) in AC6; and C162 and C174 in the Gαs CAM. These cysteines were identified as free and amenable to post-translational modification in our previous study.[32]

3.2 | Co-IP of AC6 and Gαs

To experimentally analyze the role of AC6–C2 C1004 in the interaction, we first stably co-expressed both the FLAG-tagged wild-type AC6 or the FLAG-tagged AC6 (C1004A), and HA-tagged WT Gαs in HEK293T cells. Figure 1B shows the FACS plots for the AC6 WT–Gαs WT and AC6 (C1004A)–Gαs WT stably co-expressing cells, confirming the expression stoichiometry. We then prepared the total cell lysates for the HEK293T cells stably co-expressing both AC6 and Gαs and performed co-IP using both anti-FLAG and HA beads to examine the pulldown of AC6 and Gαs in the WT and C1004A mutant. In Figure 1C, co-IP studies of AC6 WT (left panels) versus AC6 C1004A (right panels) indicated that mutating C1004 in AC6 visibly diminished the association of AC6 (IP-FLAG) with Gαs (WB-HA); however, this comparison did not achieve statistical significance due to inherent variability between co-precipitation blots (Figure S1). Mouse IgG was used as the negative control for this experiment. Co-precipitation of AC6 WT with Gαs WT was not diminished by reducing conditions (data not shown), so the formation of a covalent disulfide between C1004 in AC6 and Cys237 in Gαs cannot be imputed; only that these two cysteines appear to be involved in the intermolecular interaction necessary to activate AC6. To address the possibility that the Gαs conformation in its inactive state was affecting its interaction with the docking interface of either AC6 or AC6 C1004A, we used a GTPase-impaired CAM, Gαs Q227L. Termed here the Gαs CAM, this mutant remains GTP-bound, resulting in the maintenance of an active state with the correct switch II conformation for interaction with AC. Figure 1D shows co-IP of AC6 WT or AC6 C1004A with Gαs Q227L; similar to the WT Gαs data, mutation of AC6 C1004 decreased the intensity of the co-precipitated band for Gαs, as visualized by antibody to HA. This comparison was statistically significant ($p<0.001$). Densitometric analyses of co-IP blots are presented in Figure S1.

3.3 | Mutation of cysteine residues in AC6 affects AC activity and cAMP generation

ACs are activated in response to the occupation of Gαs at their binding sites.[47] Intracellular cyclic AMP concentrations are principally controlled at the level of its synthesis, by ACs, which converts ATP into cAMP (Figure 2A). To understand the role of the predicted residues in AC6 function, we mutated the selected cysteine residues in AC6 and Gαs to alanine. First, we examined the role of cysteines in AC6 and constructed HEK293T cells stably expressing AC6 WT, AC6 (C1004A), AC6 (C1145A), and AC6 (C447A). Using previously published protocols to specifically measure ATP catalysis by AC[11] we measured the AC activity in lysates tested

FIGURE 1 Characterization of AC cysteine-to-alanine mutants. (A) Partial molecular model of human AC6–Gαs complex, based on known bovine AC9–Gαs cryoEM structure. Interactions visualized using the PyMol software: human AC6-C1 (brown), AC6-C2 (light blue), in complex with human Gαs (green). Locations of the residues C1145 and C447 in AC6, and C162 and C174 in Gαs, are highlighted. Inset shows the proximity of residues C1004 of AC6-C2 interacting with C237 in Gαs. (B) AC6-FLAG and Gαs-HA double staining by flow cytometry. The top right quadrant of each plot represents FLAG-APC and HA-Alexa fluor 488-dual-stained cells. (C) Co-immunoprecipitation of AC6 WT with Gαs WT (left) and AC6 (C1004A) with Gαs WT (right), stably co-expressed in HEK293T cells. (D) Co-immunoprecipitation of AC6 WT with Gαs CAM (left) and AC6 (C1004A) with Gαs CAM (right), stably co-expressed in HEK293T cells. Two hundred fifty micrograms of total lysate protein was immunoprecipitated using antibody to FLAG tag (AC6) or to HA tag (Gαs), then separated by SDS-PAGE and transferred to nitrocellulose for western blotting. Lane 1 shows the molecular weight ladder (L); Lane 2 shows proteins immunoprecipitated using anti-FLAG antibody; Lane 3 proteins immunoprecipitated using anti-HA antibody; Lane 4 proteins immunoprecipitated using IgG (negative control); Lane 5 is the input (100 μg). The upper part of the blot was probed with anti-FLAG antibody and the lower part was probed with anti-HA antibody. These blots are representative of at least three independent experiments. Quantitative comparison of band densities shown in Supplementary Figures. AC, adenylyl cyclase; CAM, constitutively active mutant; SDS-PAGE, sodium dodecyl sulfate-polyacrylamide gel electrophoresis

against serial concentrations of ATP: AC6 WT, EC_{50}: 9.7 ± 3.8 μM, E_{max}: 4019 ± 591 (ΔF/mg/min); AC6 (C1004A), EC_{50}: 5.3 ± 0.6 μM, E_{max}: 1724 ± 410 (ΔF/mg/min); AC6 (C1145A), EC_{50}: 6.2 ± 0.1μM, E_{max}: 2771 ± 536 (ΔF/mg/min); AC6 (C447A), EC_{50}: 20.1 ± 1.5 μM, E_{max}: 3266 ± 768 (ΔF/mg/min) (Figure 2B,C). We observed a statistically significant decrease in AC activity at 1 mM ATP for AC6 (C1004A) (Figure 2C, $p < 0.001$). We then measured cAMP accumulation in live HEK293T cells stably expressing AC6 WT or the cysteine mutants under basal conditions without exogenous ATP. Only AC6 (C1004A) demonstrated a significant decrease in intracellular cAMP ($p < 0.05$) (Figure 2D). We confirmed that these results were not due to change in AC expression, by western blot (Figure 2E) and intracellular FACS analysis (Figure 2F) showing no significant differences in FLAG-tagged AC6 expression between the WT and mutants.

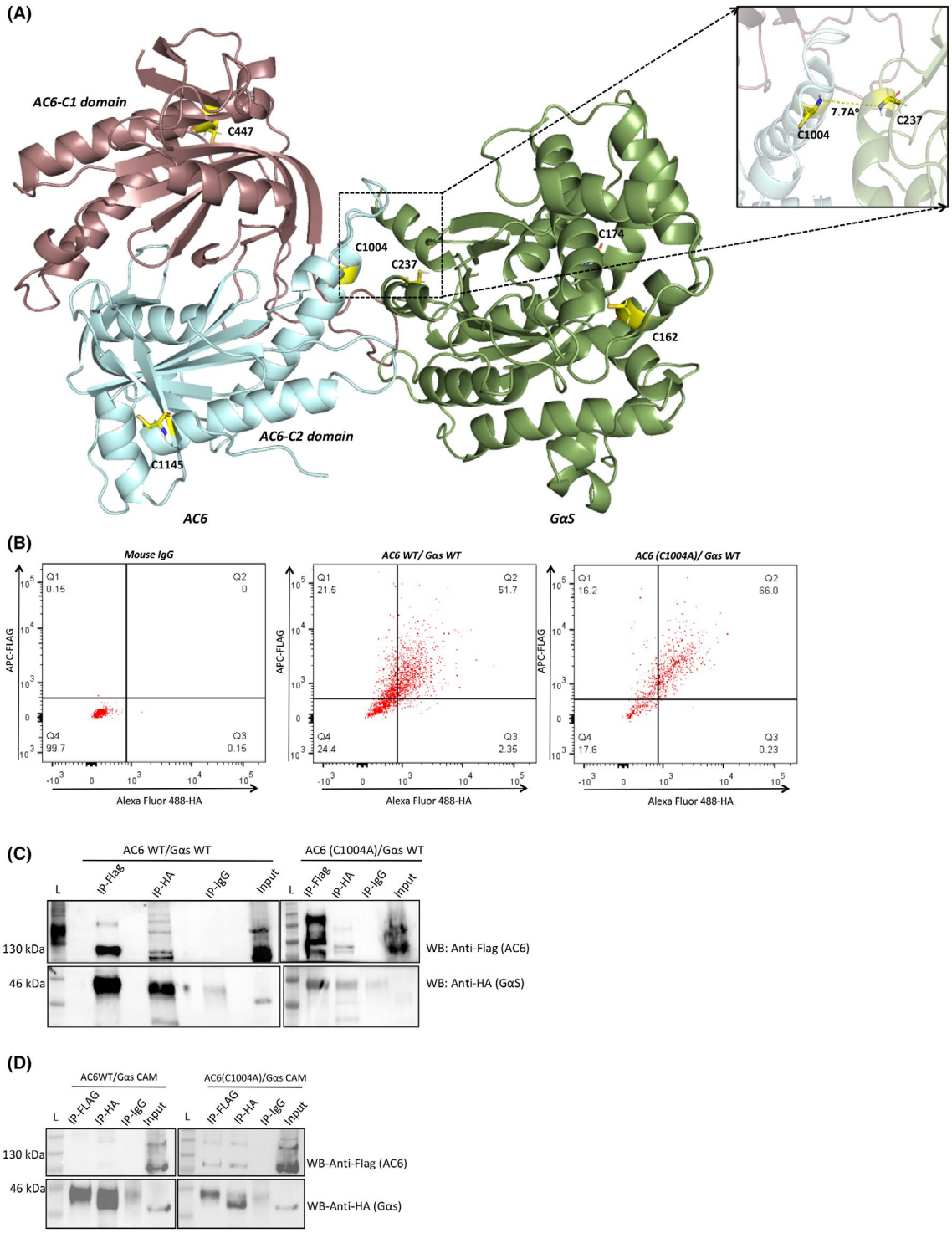

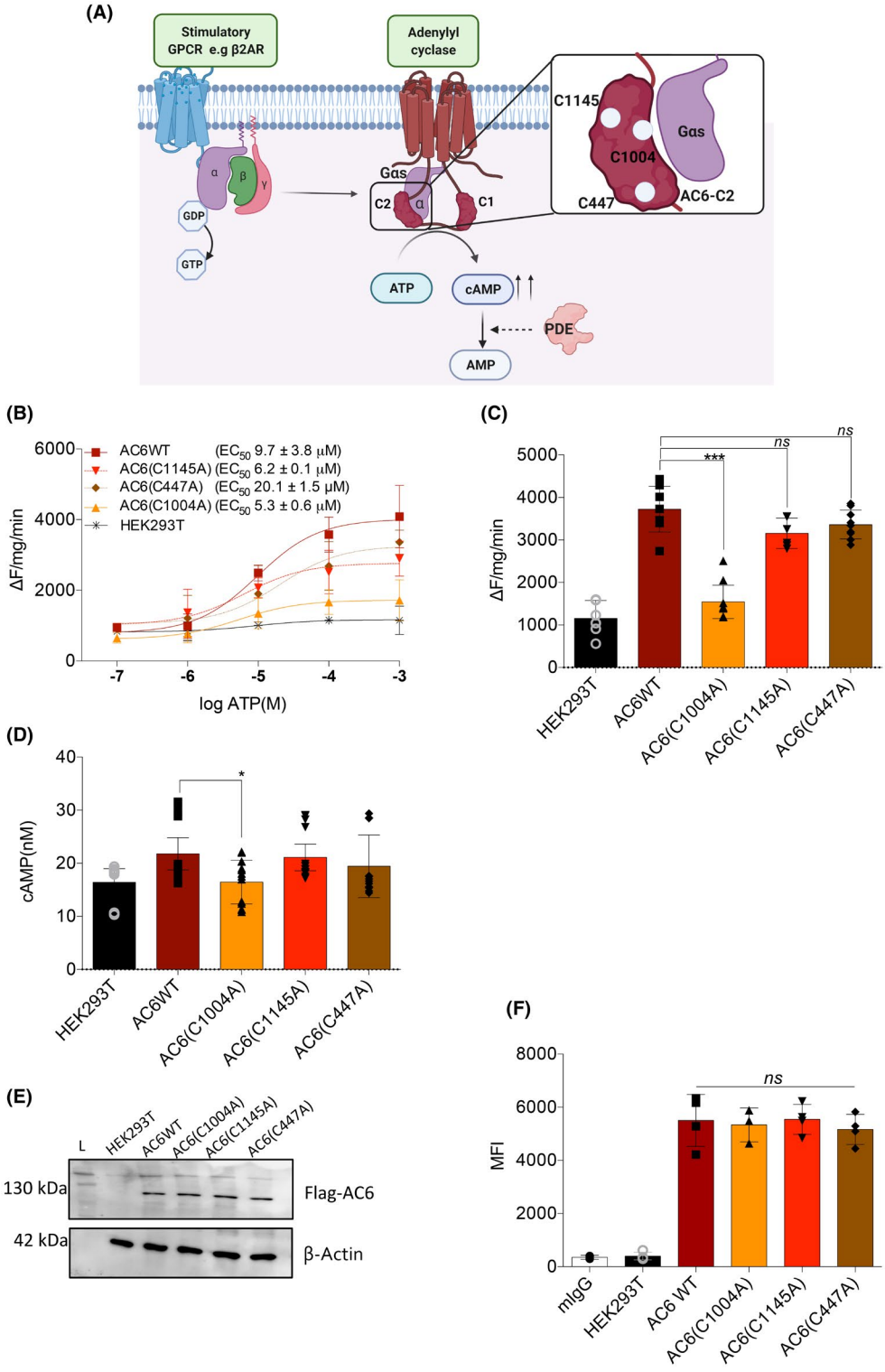

3.4 | Cysteine mutation in Gαs at C237A influences activation of AC6

After mutational analysis of AC6-side cysteines, we transitioned to study Gαs cysteines. To examine Gαs activation of AC6 independent of the need for receptor stimulation, we employed Gαs containing a mutation at Q227L in the GTPase domain (Figure 3A), referred to as Gαs CAM. The Gαs CAM exhibits reduced GTPase activity and increased AC activation[33,34] and has been used previously to examine the interaction between AC and Gαs.[48,49] We did not observe any significant conformational differences between Gαs WT and CAM upon close analysis of the homology models (Figure S2). As expected, in Figure 3B,C, HEK293T cells stably expressing the Gαs CAM exhibit higher basal cAMP production

FIGURE 2 Effect of AC cysteine to alanine mutations on AC6 function. (A) Schematic figure showing Gαs interaction with AC, AC activation and the generation of intracellular cAMP. Cysteines targeted for mutational analysis are located on the cartoon as white dots (representative figure, not drawn to scale). (B) AC catalytic activity quantified in lysates as the loss of terbium-norfloxacin fluorescence (ΔF/mg total protein/time) in the presence of serial concentrations of substrate ATP. (C) AC activity at 1 mM ATP (ΔF/mg/min). (D) Live cell cAMP generation in agonist-naïve HEK293T, expressing AC6WT or cysteine mutants, obtained using cAMP Glo Max assay kit, shown as cAMP in nM. (E) Western blot of AC6 expression in 40 μg of membrane enriched proteins from HEK293T cells stably expressing AC6WT and cysteine mutants, separated using SDS-PAGE. The blots were probed with rabbit monoclonal anti-FLAG antibody (1:1000). HEK293T cells not expressing a FLAG-tagged protein were used as antibody control; β-actin used as the loading control. (F) Protein expression quantified by FACS analysis of HEK293T, FLAG-tagged AC6 WT and mutants shown as mean fluorescence intensity values. Data indicate mean ± SEM obtained from at least three independent experiments. All statistical comparisons by one-way ANOVA with Dunnet's post hoc test for multiple comparisons, versus AC6 WT. $*p < 0.05$, $***p < 0.001$; ns, non-significant. AC, adenylyl cyclase; ANOVA, analysis of variance; cAMP, cyclic adenosine monophosphate; FACS, fluorescence activated cell sorting; SDS-PAGE, sodium dodecyl sulfate-polyacrylamide gel electrophoresis; SEM, standard error of the mean

as well as AC activity as compared to the Gαs WT. Figure 3D shows the western blot for protein abundance of Gαs WT and CAM.

To examine the functional importance of cysteine residues, we then transiently transfected HEK293T cells with Gαs WT, Gαs CAM, or Gαs CAM containing cysteine-to-alanine mutations at the predicted sites (C237A, C162A, and C174A), hereafter referred to as Gαs CAM (C162A), Gαs CAM (C174A), and Gαs CAM (C237A).

We first examined the effect of cysteine mutations in Gαs upon cAMP accumulation and observed that in both the basal unstimulated condition, as well as upon stimulation with allosteric AC activator forskolin. Cells expressing Gαs CAM (C237A) or Gαs CAM (C162A) showed a significant decrease in intracellular cAMP generation by endogenous AC, as compared to cells expressing Gαs CAM (Figure 4A). In contrast, Gαs CAM (C174A) did not alter cAMP accumulation. Next, we examined the effect of cysteine mutations in Gαs CAM on AC catalytic activity in cell lysates stimulated with exogenous ATP. Selecting only those Gαs residues that exhibited an effect on cAMP accumulation we transiently transfected HEK293T cells with pcDNA (control), Gαs WT, Gαs CAM, Gαs CAM (C237A), or Gαs CAM (C162A). As shown in Figure 4B, there was no significant change in AC activity between Gαs CAM and Gαs CAM (C162A); however, the Gαs CAM (C237A) mutant exhibited a statistically significant decrease in AC activity ($p < 0.01$). Equivalent HA-tagged Gαs protein expression in the transiently transfected cells was confirmed by western blot (Figure 4C); no significant difference in expression was observed between the Gαs CAM and its cysteine mutants (Figure S3).

To determine whether cysteine mutations in Gαs alter its activating effect on AC6, we used HEK293T cells stably expressing AC6 WT or AC6 (C1004A), then transiently transfected these stable cells with pcDNA (control), Gαs WT, Gαs CAM, or the Gαs CAM cysteine mutants, and examined the effect on intracellular cAMP generation. As shown in Figure 4D, both AC6WT and AC6 (C1004A) exhibited statistically significant decreases in intracellular cAMP when co-expressed with Gαs CAM (C162A), and Gαs CAM (C237A) mutants.

3.5 | Substitution of cysteine at 1004 in AC6 renders AC amenable to inhibition by Gαi

We had hypothesized that the activation of AC6 by Gαs requires interaction of C1004 in AC6 with C237 in Gαs. Data thus far showed that mutating one interacting partner residue to alanine did not affect the physical association of the two proteins but did exert significant functional effects on the catalytic activity of AC as well as on the generation of the second messenger cAMP. Mutating cysteines in Gαs at two key positions C162A and C237A resulted in decreased intracellular cAMP; however, the effect on AC activity persisted only for C237A. The function of AC6 is tightly regulated by binding to Gαs or Gαi. Binding of Gαs activates AC6 while Gαi inhibits it (Figure 5A). We then hypothesized that the cysteine mutations in AC6 could alter the relative binding of Gαs or Gαi to AC6.

To determine which cysteine mutations render the AC6 molecule more amenable to interaction with Gαi, HEK293T cells stably expressing AC6WT, AC6 (C1004A), AC6 (C1145A), and AC6 (C447A) were stimulated with 3 μM Forskolin and assayed for Gαi-mediated AC inhibition, detected as a downward deflection in stimulated cAMP concentration compared to the control.[50] Gαi inhibitor Tat-GPR was used to examine for reversal of Gαi-mediated inhibition. Cells were treated with Tat-GPR for 20 min at 100 nM.[42,51] In Figure 5B, data are shown as raw cAMP values in picomoles (pM). Diminution of forskolin-stimulated cAMP due to the action of Gαi was significantly greater for AC6 (C1004A) as compared to AC6WT and the other cysteine mutants. Upon treatment with Gαi inhibitor, cAMP accumulation by only AC6 (C1004A) increased, though not fully restored to levels generated by WT AC6. This increase in cAMP between AC6 (C1004)

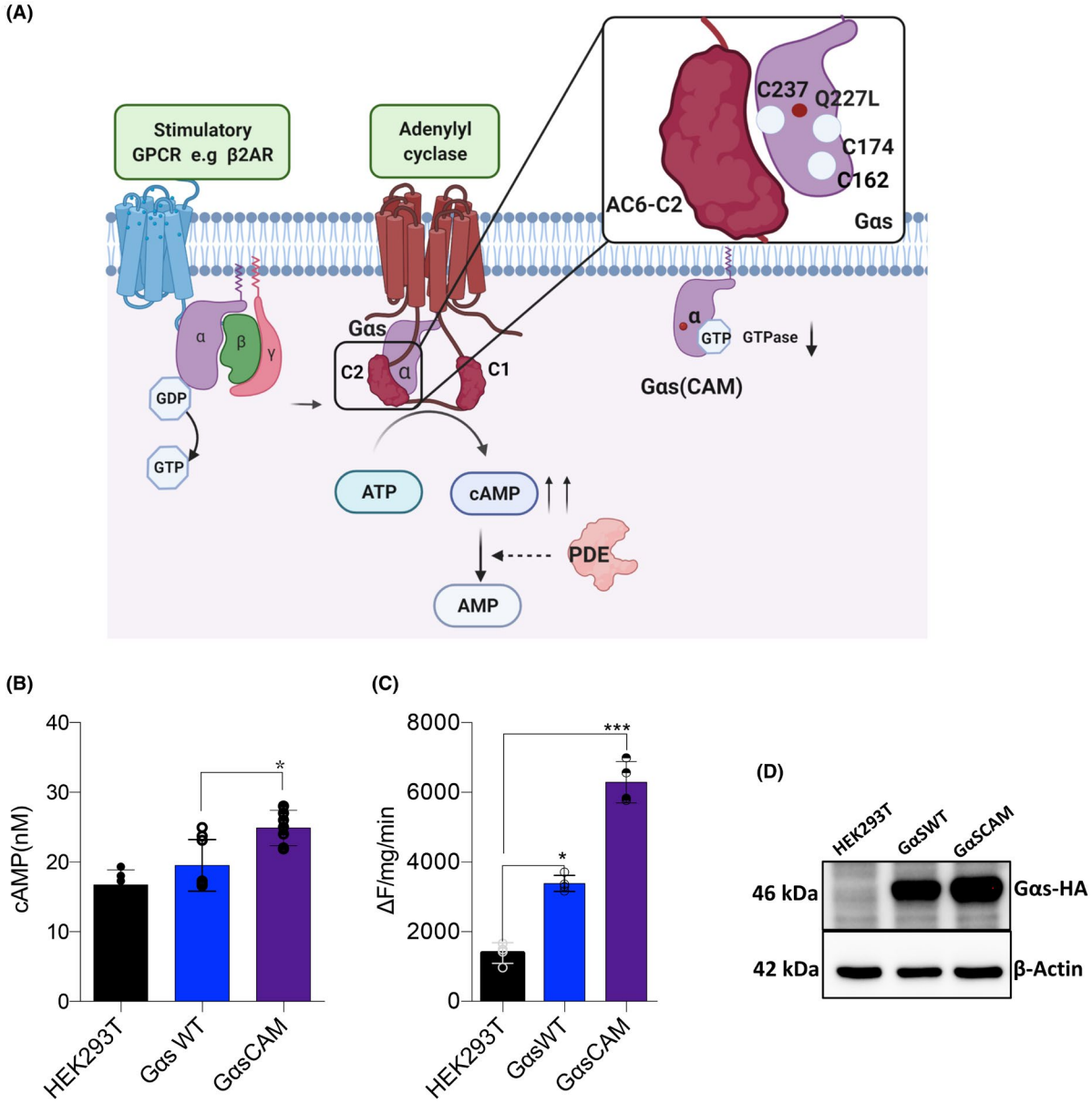

FIGURE 3 Effect of Gαs CAM cysteine to alanine mutations on AC6 activity. (A) Schematic figure showing the interaction of Gαs CAM (Q227L) mutant with AC. Gαs cysteines targeted for mutational analysis are located on the cartoon as white dots; Q227L mutation conferring constitutive activity shown as a red dot (representative figure, not drawn to scale). (B) Intracellular cAMP generation in agonist-naïve HEK293T, expressing Gαs WT, or Gαs CAM (Q227L), obtained using live cell cAMP Glo Max assay kit, shown as cAMP in nM. (C) AC catalytic activity quantified as the loss of terbium norfloxacin fluorescence (ΔF) at 1 mM ATP (ΔF/mg/min). (D) Western blot for Gαs WT and Gαs CAM (Q227L) in 40 μg of total cell lysates prepared from HEK293T cells, HEK293T stably expressing Gαs WT, or Gαs CAM, following separation using SDS-PAGE. The blots were probed with mouse monoclonal anti-HA antibody (1:1000). HEK293T cells not containing a HA-tagged protein were used as antibody control; β-actin as the loading control. All statistical comparisons by one way ANOVA using Dunnet's post-hoc test. *$p < 0.05$, ***$p < 0.001$; ns, non-significant. ANOVA, analysis of variance; CAM, constitutively active mutant; cAMP, cyclic adenosine monophosphate; SDS-PAGE, sodium dodecyl sulfate-polyacrylamide gel electrophoresis; SEM, standard error of the mean

and Tat-GPR-treated AC6 (C1004A) was statistically significant ($p < 0.01$).

To confirm this, we performed a pulldown assay using FLAG-tagged beads in whole lysates of HEK293T cells stably expressing AC6WT, AC6 (C1004A), or AC6 (C1145A). We then probed the blots with anti-FLAG, anti-Gαs, or anti-Gαi antibodies. In Figure 5C, AC6 (C1004) exhibits relatively significantly higher association with Gαi as compared to AC6WT and AC6 (C1145A), while its co-precipitation with Gαs is lesser than others. We, therefore, infer that a cysteine mutation at the 1004 position renders AC6 amenable to inhibition by Gαi. Western blots of the

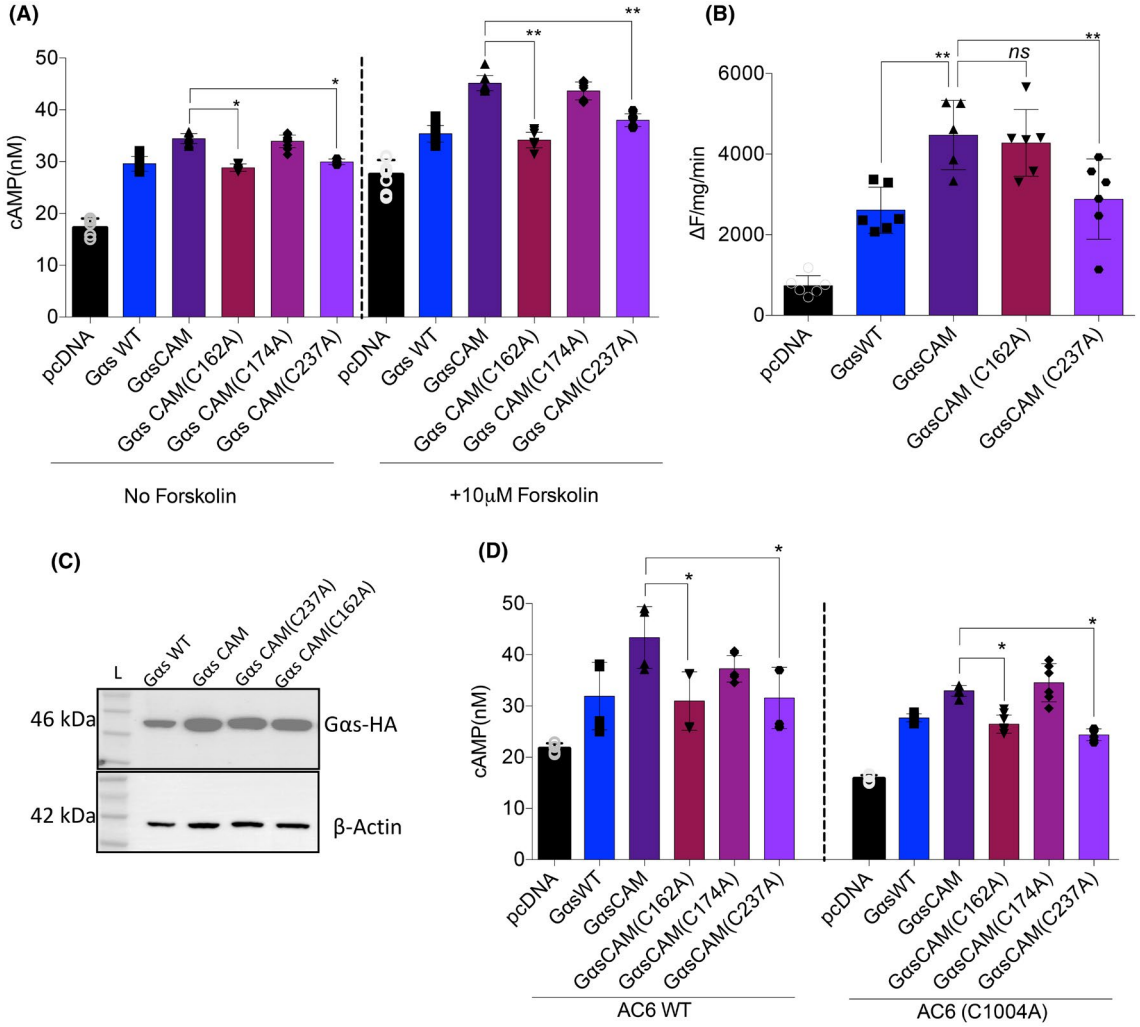

FIGURE 4 Analysis of cysteine to alanine mutations in Gαs. (A) Intracellular cAMP generated in HEK293T transiently transfected with pcDNA (control), Gαs WT, Gαs CAM (Q227L), or Gαs CAM containing cysteine mutants C162A, C174A, or C237A, at basal level (left) or after stimulation with forskolin (allosteric AC activator; 10 μM). Results obtained using live cell cAMP Glo Max assay kit, shown as cAMP in nM. (B) Unstimulated AC activity in HEK293T cells transiently transfected with pcDNA (control), Gαs WT, Gαs CAM, Gαs CAM (C162A) or Gαs CAM (C237A), quantified as the loss of terbium norfloxacin fluorescence (ΔFI) at 1 mM ATP (ΔF/mg/min). (C) Western blot of HEK293T cells transiently transfected with Gαs WT, Gαs CAM, Gαs CAM (C162A) or Gαs CAM (C237A), confirming abundance of the overexpressed proteins. Total cell lysates separated using SDS-PAGE; 40 μg protein used for western blotting. The blots were probed with mouse monoclonal anti-HA antibody (1:1000); β-actin was used as the loading control. Representative of at least three independent experiments. Quantitative comparisons of band densities are shown in Supplementary Figures. (D) Intracellular cAMP generation in HEK293T cells stably expressing AC6 WT (left panel) or AC6 (C1004A) (right panel), transiently transfected with Gαs WT, Gαs CAM (Q227L), and the cysteine mutants Gαs CAM (C162A), Gαs CAM (C174A) or Gαs CAM (C237A), obtained using live cell cAMP GloMax assay kit, shown as cAMP in nM. All statistical comparisons by one way ANOVA against Gαs CAM, using Dunnet's post-hoc test for multiple comparisons. *$p < 0.05$, **$p < 0.01$; ns, non-significant. AC, adenylyl cyclase; ANOVA, analysis of variance; CAM, constitutively active mutant; cAMP, cyclic adenosine monophosphate; SDS-PAGE, sodium dodecyl sulfate-polyacrylamide gel electrophoresis

whole lysates pre-immunoprecipitation shown as controls (Figure 5D), confirming comparable abundance of FLAG-tagged AC6 in WT and mutants as well as native AC6, Gαs and Gαi abundance in naïve HEK293T cells. Quantification of densitometry for FLAG-immunoprecipitated AC6, Gαi, and Gαs as well as for the native AC6, Gαi, Gαs, and β actin is presented in Figure S4.

4 | DISCUSSION

This study focused on identifying regulatory cysteines in AC6, the most abundant and functionally significant AC isoform in pulmonary arterial myocytes,[16] examining the interaction between AC6 and Gαs using mutational studies as well as functional assays in HEK293T cells. We have

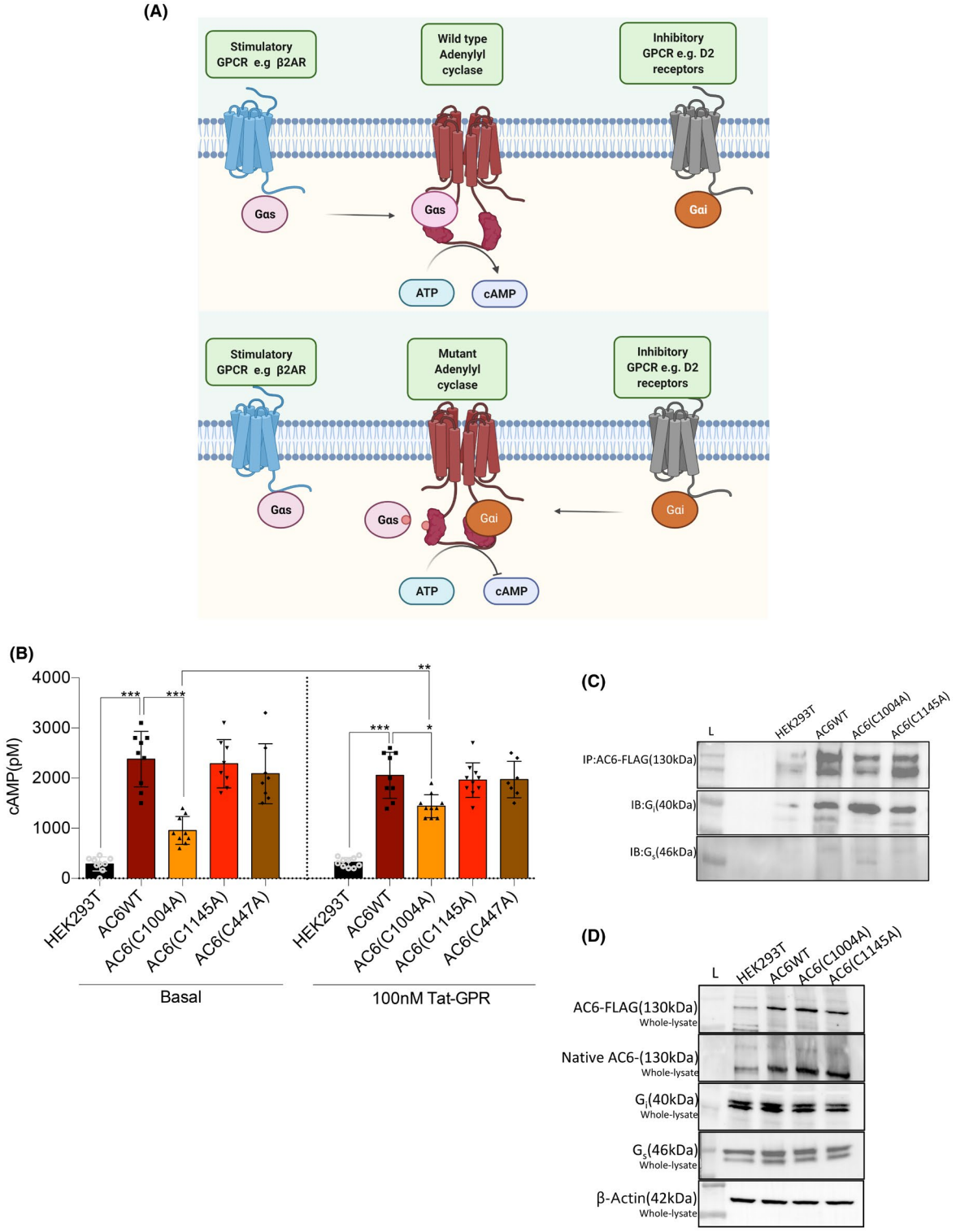

previously shown that the Gαs-mediated activation of AC6 is significantly decreased in hypoxic pulmonary artery myocytes, coincident with increased cysteine nitrosylation of AC6.[16] Analyses of AC5 have shown that cysteines in its C1 and C2 domain are important for its catalytic as well as regulatory functions.[22] These cysteines are also conserved across other AC isoforms; AC5 has the greatest sequence homology with AC6 (91.5% pairwise sequence alignment score).

We had previously modeled the interaction between AC6 and Gαs using homology modeling,[32] and concluded that the activation of AC6 by Gαs was hinged on a single nitrosylatable cysteine in each protein within close proximity. Functional domains in ACs are highly conserved, hence in this study we first revised our homology model for AC6–Gαs interaction using the cryoelectron microscopy structure reported in 2019 for bovine AC9 bound to

FIGURE 5 Effect of AC cysteine-to-alanine mutation on G-protein coupling. (A) Schematic figure showing the regulation of AC activity via Gαs and Gαi, and effect of AC6 (C1004A) on the balance of Gs/Gi regulation. Figure is representative, not drawn to scale. (B) Gi mediated cAMP generation measured using homogeneous time-resolved fluorescence (HTRF)-based cAMP kit (CisBio); 2500 cells/well were added in triplicate wells in white 96-well plates (low-volume white microplate) in the absence or presence of 3 μM forskolin. FRET ratios (665/615 nm) measured using Flex station 3 plate reader (Molecular Devices) were extrapolated to cAMP concentrations (in pM) using a standard curve, per manufacturer's recommendations. This assay was repeated at least three times, and comparisons made using one-way ANOVA with Dunnet's post-hoc test. $*p < 0.05$, $**p < 0.01$, $***p < 0.001$; ns, non-significant. (C) HEK293T cells stably expressing FLAG-tagged AC6 WT, AC6 (C1004A) or AC6 (C1145A) were lysed before immunoprecipitation of 250 μg total protein with antibody to FLAG. Co-precipitated AC6-associated proteins were separated on SDS polyacrylamide gels and transferred to nitrocellulose for western blotting. Upper blot probed with anti-FLAG antibody; middle blot probed with anti-Gαs antibody; lower blot probed with anti-Gαi antibody. Lysed native HEK293T cells were used as antibody control. L = molecular weight ladder. (D) Whole lysate abundance of AC6-FLAG, native AC6, Gαs, Gαi, and β-actin proteins. Quantitative comparison of band densities shown in Supplementary Figures. ANOVA, analysis of variance; cAMP, cyclic adenosine monophosphate; SDS-PAGE, sodium dodecyl sulfate

Gαs.[21] The cysteines predicted to be amenable to nitrosylation remained conserved between AC6 and AC9. While the orientation of Gαs in the docked model changed based on the newly defined AC9-Gαs structure, the residues in AC6 predicted to be relevant to Gαs interaction remained the same. We, therefore, carried out site-directed mutagenesis of AC6 (C1004) and Gαs (C237) using cysteine-to-alanine substitution. We also mutated other (predicted) nitrosylatable residues close to and distant from the interaction site, to rule out accessory involvement and to act as controls. Native cell systems such as pulmonary arterial myocytes express several ACs which could complicate the mutational analysis of one specific isoform, thus we chose HEK293T cells as the heterologous cell expression system. While HEK293T does express AC isoforms endogenously,[52] in our hands their background AC activity is low enough to be readily distinguishable from overexpressed AC.

We then examined the AC activity of AC6WT as well as all the AC6 cysteine mutants. We observed that at equivalent protein expression levels, with varying concentrations of substrate ATP, AC6 (C1004A) exhibited significantly lower basal (unstimulated) activity than WT and generated a significantly decreased amount of intracellular cAMP. C1004 is located on the solvent-exposed surface of the highly conserved C2 domain in AC6 close to the ATP binding site, and adjacent to the Gαs insertion point at the groove formed by two alpha helices in C2 domain of AC6. C1004 corresponds to the C911 located in AC2 previously shown to be key for interaction with Gαs.[53] It is likely that mutating such a key cysteine weakens the C1–C2 clamping and thus ATP binding required for AC activation, which could explain the reduced activation by endogenous Gαs and thus the decreased AC activity and cAMP.

We next characterized the other interaction partner, Gαs. The activation of Gαs is highly dependent on receptor stimulation, such that wild-type Gαs would need to be co-expressed with a cognate G-protein coupled receptor; this complicates unstimulated functional assays examining the interaction of Gαs with AC.[54] HEK293T cells also express high basal cAMP,[55] which may obscure the effect of site-directed mutations in Gαs. Thus, to abolish the need for an affiliated receptor as well as to clearly delineate functional effects of the cysteine mutants, we employed the CAM of Gαs (Gαs CAM) which contains a mutation in the phosphodiesterase domain (Q227L) preventing the hydrolysis of bound GTP, resulting in high basal activity.[34] We confirmed both the expression and the AC-stimulating activity of Gαs CAM as compared to the Gαs WT in HEK293T cells stably expressing these proteins. We then performed site-directed mutagenesis in the Gαs CAM, targeting nitrosylatable cysteines proximal or distal to the predicted AC interaction site. We observed that AC-mediated live cell cAMP production was significantly reduced for both Gαs CAM (C162A) and Gαs CAM (C237A), under both basal and forskolin-stimulated conditions. However, AC catalytic activity (determined as loss of ATP-bound lanthanide fluorescence, an indirect but specific indicator of AC ATPase activity[44]) was significantly reduced only for Gαs CAM (C237A). These data suggested that C237 in Gαs is required for AC catalysis of ATP. We then transfected the Gαs WT and CAM mutants into HEK293T cells stably expressing AC6 or AC6 (C1004A). Similar results were obtained: live cell cAMP production was significantly reduced for both Gαs CAM (C162A) and Gαs CAM (C237A) transfected cells. While the lanthanide-based AC activity measures substrate ATP turnover and is an assessment of AC catalytic function, the intact cell cAMP assay is a cumulative measure of product formation in the absence of exogenous substrate, reflecting a steady state inclusive of cAMP generation, degradation, or export.[24] Our data indicate that while both C162 and C237 may be important for Gαs activity, only C237 is critical for (Gαs-mediated) activation of AC. Upon close examination of the homology model of AC6–Gαs, C162 is located much further from the interaction site and is

buried in the alpha helix of Gαs close to glutamic acid at 176 position. Mutating C162 to a non-polar alanine may affect the interaction between these two residues, altering protein structure; our preliminary in silico mutagenesis of C162A suggested a conformational change from the Gαs CAM homology model with root-mean-square deviation of 3.05 Å, a value large enough to suggest a perturbation in protein configuration.[56] While we speculate that this could explain the impact of a C162 mutation on the binding of Gαs to AC, further structural data is needed to robustly clarify this finding.

Mutation of AC at C1004 did indeed inhibit baseline AC6 activity and cAMP generation, relative to AC6 WT or to AC6 mutated at other cysteine positions. Per our initial hypothesis, mutation of AC6 at C1004 should decrease the physical association of AC6 (C1004A) with Gαs WT, impairing activation of AC(C1004A). While substitution of AC6 C1004 appeared to only modestly inhibit AC6 association with Gαs WT, the importance of this cysteine was clarified upon co-precipitation with Gαs CAM, demonstrating a significant loss of association between AC6 C1004A and active state Gαs. Disulfide bond formation is not postulated, as reducing conditions did not abolish co-precipitation of AC6 with Gαs. In the absence of covalent bonds, it is known that pulldown binding assays may underestimate reversible interactions between AC and other binding proteins.[57] The observed decrease in interaction could owe to conformational changes in the AC6 molecule; loss of sequential binding could also give rise to conformational changes altering intermolecular interactions. A molecular dynamics study of AC5–Gαs interaction showed that the C2 domain of AC5 can undergo three different conformations involving large movement of the β2 loop,[58] such that the conformation of AC5 initially docked with Gαs differs from the activated, Gαs-plus-ATP-bound AC5 conformation. A model of AC9–Gαs interaction also demonstrated a secondary conformational change largely mediated by binding of ATP.[21] These sequential conformational changes are intrinsic to AC regulation; AC5 bound to Gαs is inimical to AC5 binding to Gαi, while dissociation of Gαs renders AC5 accessible for Gαi binding.[59] We speculate that AC6 C1004 is required for its interaction with Gαs to trigger the conformational change of AC6 to its active ATPase state.

The activity of AC isoforms are differentially regulated by stimulatory and inhibitory G proteins.[14] Group III ACs AC5 and AC6 are classically activated by Gαs or Gβγ,[60] while regulated negatively by Gαi,[14] calcium[61] and protein kinases.[30,31,62] Gβγ interactions with AC6 and AC5 require initial Gαs binding, and can also augment forskolin-mediated activation[63]; but Gβγ binding to AC5 and to AC6 are differently regulated despite the structural similarity of these two AC isoforms, highlighting the relevance of individual residues governing these specific molecular interactions.[57] To determine the residues critical for the regulatory balance of G-protein interaction, we examined the association of AC6 WT or AC6 cysteine mutants with Gαs and Gαi by co-IP, and found that mutation of C1004 resulted in greater association with Gαi and diminished association with Gαs. Additionally, measured cAMP production by AC6 became more amenable to inhibition by Gαi. This was partially reversed upon treatment with cell-permeable Gαi inhibitor Tat-GPR. The Tat-GPR peptide inhibits only Gαi while stimulating the activation of Gβγ signaling, while pertussis toxin inhibition stabilizes the entire heterotrimer.[42,51] Its high specificity and efficiency depend on the presence of the GPR motif in $G\alpha i_{1\text{-}3}$ isoforms, which functions as a guanine nucleotide dissociation inhibitor.[51] This peptide blocker has low affinity for Gαi family members Go or Gz, so we recognize some AC-inhibitory signal may remain despite its usage.[64] Studies in AC5 have shown that Gαs and Gαi can bind distinct domains of AC to elicit their effect.[65] The conformational state of the C1 and the C2 domains are critical for AC function. Gαs subunit binds to C2 (in the cleft formed by the α2' and α3' helices)[47,53] and increases the affinity of the C1 and C2 domains, promoting catalysis; while Gαi binds to C1 in a similar groove[53] but counteracts AC activation.[66] Gαi mediates its inhibitory effect by reducing the ability of the C1 and the C2 domains to obtain a closed conformation, even in the presence of the allosteric activator forskolin.[65] We did not observe a complete loss of Gαs binding to AC6 (C1004A), suggesting that Gαs and Gαi regulate AC function in a ratio dependent manner. The absence of AC6 C1004 could result in a conformation favoring the binding of Gαi while not completely abolishing binding of Gαs. A study of inhibition of AC5 by Gαi showed that an activated Gαi clamps the C1 cytosolic domain into inactive conformation.[67] AC can simultaneously bind to both stimulatory and inhibitory G proteins creating binary or ternary complexes; in any combination inclusive of a Gαi, the AC structure is modified to an inactive conformation with diminished ATP binding probability, even if a stimulatory Gα also forms part of that complex.[68] We speculate that C1004 may be required to stabilize the exclusive AC6–Gαs interaction, such that its absence permits AC6 to simultaneously associate with Gαi, resulting in a conformation repressing ATP catalysis.

In summary, our data identify key roles for free cysteines C1004 in AC6, and C237 in Gαs, for the activation of AC6. While cysteines present at solvent-exposed surfaces are known to play key roles in protein stability, their role in reversible protein-protein interactions has

been less explored and further structure/function studies are warranted. Free cysteines are amenable to several post-translational modifications depending upon the cellular environment. Building on our previous report that agonist-naïve and agonist-stimulated AC6 activity in hypoxic myocytes is inhibited due to S-nitrosylation occurring at very specific cysteines,[16] the present study suggests a possible mechanism for AC inhibition by cysteine unavailability due to post-translational modification, by using mutational analysis to confirm the critical residues for AC interaction with Gαs, the absence of which appear to free AC6 for an inhibitory interaction with Gαi.

ACKNOWLEDGMENTS

This project was supported by operating grant from Heart and Stroke Foundation of Canada (SD); fellowship to AYB from Research Manitoba/Children's Hospital Foundation of Manitoba.

CONFLICT OF INTEREST

Neither this manuscript nor any part of it has been previously published; it is not currently under consideration for publication by any other journal. All co-authors have read and approved of the manuscript in its current form and agree with its submission to *FASEB Bioadvances*; they have no conflicts of interest or financial relationships to disclose.

AUTHOR CONTRIBUTIONS

Anjali Y. Bhagirath designed and performed experiments, analyzed data, designed figures, and wrote the first draft of the manuscript; Vikram Bhatia designed and performed experiments, and analyzed data; Manoj Reddy Medapati designed and performed experiments, and analyzed data; Nisha Singh designed and performed experiments; Martha Hinton designed and performed experiments; Prashen Chelikani designed experiments, analyzed data and edited the manuscript; Shyamala Dakshinamurti designed experiments, analyzed data, edited and finalized the manuscript.

ORCID

Prashen Chelikani https://orcid.org/0000-0003-1129-7957
Shyamala Dakshinamurti https://orcid.org/0000-0001-7279-5226

REFERENCES

1. Dakshinamurti S. Pathophysiologic mechanisms of persistent pulmonary hypertension of the newborn. *Pediatr Pulmonol*. 2005;39(6):492-503.
2. Baczynski M, Ginty S, Weisz DE, et al. Short-term and long-term outcomes of preterm neonates with acute severe pulmonary hypertension following rescue treatment with inhaled nitric oxide. *Arch Dis Child*. 2017;102(6):F508-F514.
3. Barrington KJ, Finer N, Pennaforte T. Inhaled nitric oxide for respiratory failure in preterm infants. *Cochrane Database Syst Rev*. 2017;1(1):CD000509.
4. Kinsella JP, Abman SH. Controversies in the use of inhaled nitric oxide therapy in the newborn. *Clin Perinatol*. 1998;25(1):203-217.
5. Bhatia V, Elnagary L, Dakshinamurti S. Tracing the path of inhaled nitric oxide: biological consequences of protein nitrosylation. *Pediatr Pulmonol*. 2020;56:525-538.
6. Schermuly RT, Inholte C, Ghofrani AH, et al. Lung vasodilatory response to inhaled iloprost in experimental pulmonary hypertension: amplification by different type phosphodiesterase inhibitors. *Respir Res*. 2005;6:76.
7. Schindler MB, Hislop AA, Haworth SG. Postnatal changes in response to norepinephrine in the normal and pulmonary hypertensive lung. *Am J Respir Crit Care Med*. 2004;170(6):641-646.
8. Lohse MJ, Hofmann KP. Spatial and temporal aspects of signaling by G-protein-coupled receptors. *Mol Pharmacol*. 2015;88(3):572-578.
9. Structure HJH. Mechanism, and regulation of mammalian adenylyl cyclase. *J Biol Chem*. 1999;274(12):7599-7602.
10. Kleinboelting S, Diaz A, Moniot S, et al. Crystal structures of human soluble adenylyl cyclase reveal mechanisms of catalysis and of its activation through bicarbonate. *Proc Natl Acad Sci U S A*. 2014;111(10):3727-3732.
11. Ganpat MM, Nishimura M, Toyoshige M, Okuya S, Pointer RH, Rebois RV. Evidence for stimulation of adenylyl cyclase by an activated Gs heterotrimer in cell membranes: an experimental method for controlling the Gs subunit composition of cell membranes. *Cell Signal*. 2000;12(2):113-122.
12. Gilman AG. G proteins: transducers of receptor-generated signals. *Annu Rev Biochem*. 1987;56(1):615-649.
13. Seamon KB, Padgett W, Daly JW. Forskolin: unique diterpene activator of adenylate cyclase in membranes and in intact cells. *Proc Natl Acad Sci U S A*. 1981;78(6):3363-3367.
14. Taussig R, Iniguez-Lluhi J, Gilman A. Inhibition of adenylyl cyclase by Gi alpha. *Science*. 1993;261(5118):218-221.
15. Taussig R, Tang WJ, Hepler JR, Gilman AG. Distinct patterns of bidirectional regulation of mammalian adenylyl cyclases. *J Biol Chem*. 1994;269(8):6093-6100.
16. Sikarwar AS, Hinton M, Santhosh KT, et al. Hypoxia inhibits adenylyl cyclase catalytic activity in a porcine model of persistent pulmonary hypertension of the newborn. *Am J Physiol Lung Cell Mol Physiol*. 2018;315(6):L933-L944.
17. McVey M, Hill J, Howlett A, Klein C. Adenylyl cyclase, a coincidence detector for nitric oxide. *J Biol Chem*. 1999;274(27):18887-18892.
18. Chen SC, Huang B, Liu YC, Shyu KG, Lin PY, Wang DL. Acute hypoxia enhances proteins' S-nitrosylation in endothelial cells. *Biochem Biophys Res Commun*. 2008;377(4):1274-1278.
19. Gow AJ, Farkouh CR, Munson DA, Posencheg MA, Ischiropoulos H. Biological significance of nitric oxide-mediated protein modifications. *Am J Physiol Lung Cell Mol Physiol*. 2004;287(2):L262-268.
20. Gaston B. Summary: systemic effects of inhaled nitric oxide. *Proc Am Thorac Soc*. 2006;3(2):170-172.
21. Qi C, Sorrentino S, Medalia O, Korkhov VM. The structure of a membrane adenylyl cyclase bound to an activated stimulatory G protein. *Science*. 2019;364(6438):389-394.

22. Tesmer JJ, Sunahara RK, Gilman AG, Sprang SR. Crystal structure of the catalytic domains of adenylyl cyclase in a complex with Gsalpha.GTPgammaS. *Science*. 1997;278(5345):1907-1916.
23. Zhang G, Liu Y, Ruoho AE, Hurley JH. Structure of the adenylyl cyclase catalytic core. *Nature*. 1997;386(6622):247-253.
24. Dessauer CW, Watts VJ, Ostrom RS, Conti M, Dove S, Seifert R. International union of basic and clinical pharmacology. CI. Structures and small molecule modulators of mammalian adenylyl cyclases. *Pharmacol Rev*. 2017;69(2):93-139.
25. Chen-Goodspeed M, Lukan AN, Dessauer CW. Modeling of Galpha(s) and Galpha(i) regulation of human type V and VI adenylyl cyclase. *J Biol Chem*. 2005;280(3):1808-1816.
26. Duhe RJ, Nielsen MD, Dittman AH, Villacres EC, Choi EJ, Storm DR. Oxidation of critical cysteine residues of type I adenylyl cyclase by o-iodosobenzoate or nitric oxide reversibly inhibits stimulation by calcium and calmodulin. *J Biol Chem*. 1994;269(10):7290-7296.
27. Ding Z, Kim S, Dorsam RT, Jin J, Kunapuli SP. Inactivation of the human P2Y12 receptor by thiol reagents requires interaction with both extracellular cysteine residues, Cys17 and Cys270. *Blood*. 2003;101(10):3908-3914.
28. Shpakov AO, Kuznetsova LA, Plesneva SA. Effects of thiols and sulfihydryl group blockers on the negative regulation of the adenylate cyclase signal system by biogenic amines. *Zh Evol Biokhim Fiziol*. 2000;36(4):293-297.
29. Nijjar MS, Chaudhary KC. Mechanism of adenylate cyclase activation by the rat lung cytoplasmic factors. *Mol Cell Biochem*. 1991;103(2):181-189.
30. Iwami G, Kawabe J, Ebina T, Cannon PJ, Homcy CJ, Ishikawa Y. Regulation of adenylyl cyclase by protein kinase A. *J Biol Chem*. 1995;270(21):12481-12484.
31. Lin TH, Lai HL, Kao YY, Sun CN, Hwang MJ, Chern Y. Protein kinase C inhibits type VI adenylyl cyclase by phosphorylating the regulatory N domain and two catalytic C1 and C2 domains. *J Biol Chem*. 2002;277(18):15721-15728.
32. Jaggupilli A, Dhanaraj P, Pritchard A, Sorensen JL, Dakshinamurti S, Chelikani P. Study of adenylyl cyclase-GalphaS interactions and identification of novel AC ligands. *Mol Cell Biochem*. 2018;446(1-2):63-72.
33. Graziano MP, Gilman AG. Synthesis in *Escherichia coli* of GTPase-deficient mutants of Gs alpha. *J Biol Chem*. 1989;264(26):15475-15482.
34. Masters SB, Miller RT, Chi MH, et al. Mutations in the GTP-binding site of GS alpha alter stimulation of adenylyl cyclase. *J Biol Chem*. 1989;264(26):15467-15474.
35. Laskowski RA, MacArthur MW, Moss DS, Thornton JM. PROCHECK: a program to check the stereochemical quality of protein structures. *J Appl Crystallogr*. 1993;26(2):283-291.
36. Upadhyaya JD, Chakraborty R, Shaik FA, Jaggupilli A, Bhullar RP, Chelikani P. The pharmacochaperone activity of quinine on bitter taste receptors. *PLoS One*. 2016;11(5):e0156347.
37. Chakraborty R, Xu B, Bhullar RP, Chelikani P. Expression of G protein-coupled receptors in mammalian cells. *Methods Enzymol*. 2015;556:267-281.
38. Liu K, Jaggupilli A, Premnath D, Chelikani P. Plasticity of the ligand binding pocket in the bitter taste receptor T2R7. *Biochim Biophys Acta Biomembr*. 2018;1860(5):991-999.
39. Nørskov-Lauritsen L, Thomsen ARB, Bräuner-Osborne H. G protein-coupled receptor signaling analysis using homogenous time-resolved förster resonance energy transfer (HTRF®) technology. *Int J Mol Sci*. 2014;15(2):2554-2572.
40. Foster SR, Hauser AS, Vedel L, et al. Discovery of human signaling systems: pairing peptides to G protein-coupled receptors. *Cell*. 2019;179(4):895-908.e21.
41. Kimple RJ, Kimple ME, Betts L, Sondek J, Siderovski DP. Structural determinants for GoLoco-induced inhibition of nucleotide release by Galpha subunits. *Nature*. 2002;416(6883):878-881.
42. Peterson YK, Bernard ML, Ma H, Hazard S 3rd, Graber SG, Lanier SM. Stabilization of the GDP-bound conformation of Gialpha by a peptide derived from the G-protein regulatory motif of AGS3. *J Biol Chem*. 2000;275(43):33193-33196.
43. Chelikani P, Reeves PJ, Rajbhandary UL, Khorana HG. The synthesis and high-level expression of a beta2-adrenergic receptor gene in a tetracycline-inducible stable mammalian cell line. *Protein Sci*. 2006;15(6):1433-1440.
44. Spangler CM, Spangler C, Gottle M, et al. A fluorimetric assay for real-time monitoring of adenylyl cyclase activity based on terbium norfloxacin. *Anal Biochem*. 2008;381(1):86-93.
45. Peterson LS, Stelzer IA, Tsai AS, et al. Multiomic immune clockworks of pregnancy. *Semin Immunopathol*. 2020;42(4):397-412.
46. DeCaprio J, Kohl TO. Denaturing lysis of cells for immunoprecipitation. *Cold Spring Harbor Protoc*. 2020;2020(2):098616.
47. Sunahara RK, Dessauer CW, Whisnant RE, Kleuss C, Gilman AG. Interaction of Gsalpha with the cytosolic domains of mammalian adenylyl cyclase. *J Biol Chem*. 1997;272(35):22265-22271.
48. Salim S, Sinnarajah S, Kehrl JH, Dessauer CW. Identification of RGS2 and type V adenylyl cyclase interaction sites. *J Biol Chem*. 2003;278(18):15842-15849.
49. Lazar AM, Irannejad R, Baldwin TA, et al. G protein-regulated endocytic trafficking of adenylyl cyclase type 9. *eLife*. 2020;9. doi:10.7554/eLife.58039
50. Wang T, Li Z, Cvijic ME, Zhang L, Sum CS. Measurement of cAMP for Gαs- and Gαi protein-coupled receptors (GPCRs). In: Markossian S, Sittampalam GS, Grossman A, eds. *Assay Guidance Manual*. Eli Lilly & Company and the National Center for Advancing Translational Sciences; 2017:807–826.
51. Appleton KM, Bigham KJ, Lindsey CC, et al. Development of inhibitors of heterotrimeric Gαi subunits. *Bioorg Med Chem*. 2014;22(13):3423-3434.
52. Soto-Velasquez M, Hayes MP, Alpsoy A, Dykhuizen EC, Watts VJ. A novel CRISPR/Cas9-based cellular model to explore adenylyl cyclase and cAMP signaling. *Mol Pharmacol*. 2018;94(3):963-972.
53. Tesmer JJG, Sunahara RK, Gilman AG, Sprang SR. Crystal structure of the catalytic domains of adenylyl cyclase in a complex with Gsα·GTPγS. *Science*. 1997;278(5345):1907-1916.
54. Conklin BR, Bourne HR. Structural elements of G alpha subunits that interact with G beta gamma, receptors, and effectors. *Cell*. 1993;73(4):631-641.
55. Atwood BK, Lopez J, Wager-Miller J, Mackie K, Straiker A. Expression of G protein-coupled receptors and related proteins in HEK293, AtT20, BV2, and N18 cell lines as revealed by microarray analysis. *BMC Genom*. 2011;12:14.
56. Maiorov VN, Crippen GM. Significance of root-mean-square deviation in comparing three-dimensional structures of globular proteins. *J Mol Biol*. 1994;235(2):625-634.

57. Brand CS, Sadana R, Malik S, Smrcka AV, Dessauer CW. Adenylyl cyclase 5 regulation by gbetagamma involves isoform-specific use of multiple interaction sites. *Mol Pharmacol*. 2015;88(4):758-767.
58. Frezza E, Martin J, Lavery R. A molecular dynamics study of adenylyl cyclase: the impact of ATP and G-protein binding. *PLoS One*. 2018;13(4):e0196207.
59. Frezza E, Amans TM, Martin J. Allosteric inhibition of adenylyl cyclase type 5 by G-protein: a molecular dynamics study. *Biomolecules*. 2020;10(9):1330.
60. Tong R, Wade RC, Bruce NJ. Comparative electrostatic analysis of adenylyl cyclase for isoform dependent regulation properties. *Proteins*. 2016;84(12):1844-1858.
61. Yoshimura M, Cooper DM. Cloning and expression of a Ca(2+)-inhibitable adenylyl cyclase from NCB-20 cells. *Proc Natl Acad Sci U S A*. 1992;89(15):6716-6720.
62. Kunkel MW, Friedman J, Shenolikar S, Clark RB. Cell-free heterologous desensitization of adenylyl cyclase in S49 lymphoma cell membranes mediated by cAMP-dependent protein kinase. *FASEB J*. 1989;3(9):2067-2074.
63. Gao X, Sadana R, Dessauer CW, Patel TB. Conditional stimulation of type V and VI adenylyl cyclases by G protein betagamma subunits. *J Biol Chem*. 2007;282(1):294-302.
64. Peterson YK, Hazard S 3rd, Graber SG, Lanier SM. Identification of structural features in the G-protein regulatory motif required for regulation of heterotrimeric G-proteins. *J Biol Chem*. 2002;277(9):6767-6770.
65. Dessauer CW, Chen-Goodspeed M, Chen J. Mechanism of Gαi-mediated inhibition of type V adenylyl cyclase. *J Biol Chem*. 2002;277(32):28823-28829.
66. Sadana R, Dessauer CW. Physiological roles for G protein-regulated adenylyl cyclase isoforms: insights from knockout and overexpression studies. *Neurosignals*. 2009;17(1):5-22.
67. van Keulen SC, Rothlisberger U. Exploring the inhibition mechanism of adenylyl cyclase type 5 by n-terminal myristoylated Galphai1. *PLoS Comput Biol*. 2017;13(9):e1005673.
68. van Keulen SC, Narzi D, Rothlisberger U. Association of both inhibitory and stimulatory Galpha subunits implies adenylyl cyclase 5 deactivation. *Biochemistry*. 2019;58(42):4317-4324.

SUPPORTING INFORMATION

Additional supporting information may be found in the online version of the article at the publisher's website.

How to cite this article: Bhagirath AY, Bhatia V, Medapati MR, et al. Critical cysteines in the functional interaction of adenylyl cyclase isoform 6 with Gαs. *FASEB BioAdvances*. 2022;4:180–196. doi:10.1096/fba.2021-00073